Heliyon 9 (2023) e22398

Contents lists available at ScienceDirect

Heliyon

journal homepage: www.cell.com/heliyon

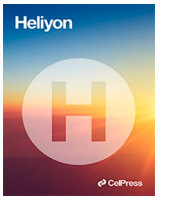

Prediction of gold mineralization zones using spatial techniques and geophysical data: A case study of the Josephine prospecting licence, NW Ghana

Eric Dominic Forson [a], Prince Ofori Amponsah [b,*]

[a] Department of Physics, School of Physical and Mathematical Sciences, University of Ghana, Accra, Ghana
[b] Department of Earth Science, School of Physical and Mathematical Sciences, University of Ghana, Accra, Ghana

ARTICLE INFO

Keywords:
Mineral prospectivity modeling
Information value
Frequency ratio
Northwestern Ghana
Geophysics dataset

ABSTRACT

In this study, predictive models that characterize gold potential zones within the Josephine Prospecting Licence (PL) Area of Northwestern Ghana have been created by data-driven methods comprising frequency ratio and information value. These predictive models were evaluated using known locations of gold (Au) occurrence datasets and compared to each other. The mineral prospectivity models (MPMs) of gold occurrence areas within the Josephine PL Area were constructed by determining the spatial correlation between known locations of Au occurrences and eight mineralization related factors. The locations of these known Au occurrences, which characterize regions of anomalously high Au geochemical concentration and regions of previous or ongoing artisanal mining operations were identified by using geographic positioning systems (GPS). Eight mineralization related factors (geoscientific thematic layers) over the entire study area composed of analytic signal, lineament density, uranium-thorium ratio, uranium, potassium-thorium ratio, potassium, reduction-to-equator and geology were used to generate the MPMs. The predictive capacity of each of the MPMs generated was determined by employing the area under the receiver operating characteristics curve (AUC). The AUC score obtained for the predictive models produced based on the information value and the frequency ratio approaches were respectively 0.794 and 0.815. The AUC scores generated indicate that the MPMs produced are good predictive models (with an AUC greater than 0.7) and can therefore assist in narrowing down the highly prospective zones of mineral occurrences within the study area. However, the overall predictive potential of the frequency ratio approach was better than the model produced by the information value approach.

1. Introduction

Predictive modeling for a particular natural resource (mineral, water etc.) entails the integration of several geospatial thematic layers sourced from various geoscientific datasets (comprising geophysical, remote sensing, geological and geochemical) with the sole objective of improving the prospect of delineating a target natural resource over an area of interest [40,66]. Thus, many exploration geoscientists in recent years have concurrently employed various statistical methods and geographic information systems (GIS) to characterize the resource potential of a specified area of interest into prospective and non-prospective zones. For example, the

* Corresponding author.
E-mail address: pamponsah@ug.edu.gh (P.O. Amponsah).

https://doi.org/10.1016/j.heliyon.2023.e22398
Received 22 June 2023; Received in revised form 2 October 2023; Accepted 10 November 2023
Available online 17 November 2023

delineation of prospective zones of a mineral deposit is very composite in nature and therefore necessitates the incorporation of extensive assessment procedures that encompass the metallogenic processes essential to the evolution of the sought-after mineral deposit [66]. The delineation of mineral prospective zones is a multicriteria decision-making problem because it also includes the selection of appropriate geoscientific criteria associated with the sought-after mineral, which are subsequently combined to produce a mineral prospectivity model (MPM). The integration of geoscientific criteria towards the production of an MPM generally comes in two flavours: knowledge-driven and data-driven methods. Knowledge-driven approaches in geoscientific data integration deal with the use of expert knowledge to assign weights to various geoscientific criteria to be employed in the generation of a predictive model. Knowledge-driven approaches that are mostly applied in the predictive modeling of a particular natural resource such as gold, copper, iron, hydrocarbons, groundwater etc. Comprise the analytical hierarchy process [34,76,84], analytical network process [68], ELECTRE [2,3], fuzzy analytical hierarchy process [14,20,45,51], best-worst method [42], PROMETHEE [4] and TOPSIS [59]. It is worthy to note that, knowledge-driven data integration methods are best suited in areas with little or no known occurrence of the sought-after mineral [45].

In the case of the data-driven methods, the weight of each of the geoscientific criteria to be used in the predictive modeling is determined by assessing how they spatially correlate with respect to known locations of the mineral occurrences within the study area [46]. The use of data-driven methods in predicting the spatial occurrence of a natural resource or a geohazard is mostly carried out by the weight of evidence [47,74], frequency ratio [16,53,69], weighting factor [9,23,35,36], statistical information [35,52], information value [6,27], shannon entropy [8,77], certainty factor [56,80], evidence belief function [40,62], neural networks [55,57], logistic regression [29,58], support vector machine [28,82], and random forest [65,80] techniques. It should also be emphasized that, data-driven methods do not work well in situations where the known locations of the sought-after mineral is limited or absent. Nevertheless, data-driven method produces optimized models in situations where substantial amount of the known mineral occurrence is present [25].

Although data-driven methods have been significantly employed for MPM in recent years, the employability of the bivariate data-driven frequency ratio (FR) technique in delineating prospective zones of mineral occurrence in Ghana and West Africa is rare in literature in spite of their proven efficacy in mapping zones of mineral occurrences in other geological terranes [16,53,69]. Regarding the information value (IV) technique, its employability is more profoundly applicable in landslide and groundwater studies [6,27]. In comparison with the multivariate data-driven methods (machine learning), the bivariate data-driven methods (including the FR and IV

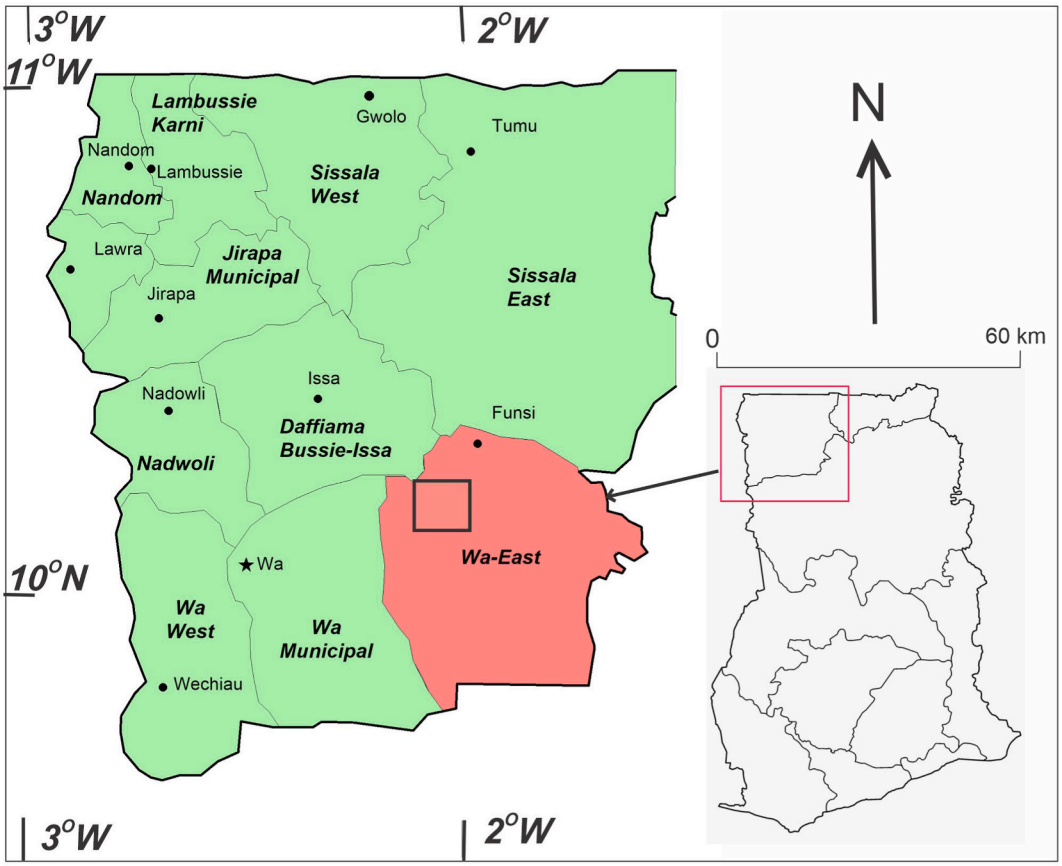

Fig. 1. Map of the northwestern Ghana showing various administrative districts (Study area is marked in black).

techniques) are simple to use with lesser computational cost and easy to interpret; provide a rapid insight into the relationship between each geoscientific criteria and known occurrences; and are less prone to overfitting, which is commonly associated with machine learning approaches [39,49,64]. Thus, the overarching objective of this study is to carry out a comparative assessment of two bivariate data-driven methods comprising the frequency ratio (FR) and information value (IV) techniques for MPM over the Josephine PL Area in Northwestern Ghana to delineate prospective zones of gold mineralization occurrence. Furthermore, the predictive models that would be produced based on the two data-driven approaches used would be evaluated to ascertain how well they performed in predicting the known Au prospects using the receiver operating characteristics (ROC) curve approach.

2. Study area and geological setting

2.1. Study area

The Josephine Tenement (Fig. 1), which hosts many prospects such as the Josephine main prospect, the Manwe NW, and the Josephine south prospects in Northwest Ghana, is about 25 km SE of Wa, the regional capital of the Upper West Region of Ghana [33]. So far, the first pass exploration programme has identified 69,000 Oz and 39,000 Oz of inferred resources on the Josephine Main and the Manwe NW prospects. Currently, exploration works are being done on the tenement by its owners, Azumah Resources Limited, to increase the gold inventory. The tenement lies in the Wa-East district and within the coordinates 569500 mE, 1109200 mN, and 579500 mE, 1094500 mN, using the UTM Zone 30 N, WGS84 Datum.

2.2. Geological context of the Josephine tenement

The Josephine PL Area located in the Upper West region of NW Ghana is part of the 2.2–2.0 Ga Birimian terrane which covers the eastern half of the southern portion of West Africa Craton (sWAC; Fig. 2(a)). The Birimian terrane [5,30,61] is composed of metamorphic greenstone belts and basins formed through accretion tectonics with long-lived sites of persistent subduction with compressional and extensional characteristics [21,37,38,48,60,67]. Unconformably overlying the southern West African Craton (sWAC) to the north is the intracratonic Neoproterozoic Taoudeni basin sediments [54,79].

NW Ghana is composed of two cratonic blocks juxtaposed with each other by two main crustal shear zones that meet at a tangential interface in NW Ghana [12,22]. The western block is mainly controlled by north-south Jirapa shear zones and the eastern block is characterized by northeast-southwest Bole-Nangodi shear zones (Fig. 2(b)). The eastern block is defined by three domains mainly as a result of an E-W splay off the Jirapa shear zone known as the Jang fault. These domains are known as the Koodougou-Tumu domain, the Julie belt and the Bole-Bulenga domain. The western block is characterized by the Wa-Lawra belt with a major N–S structural grain and marks the southern extension of the larger Boromo belt which extends into Burkina Faso. The Wa-Lawra belt is composed of metamorphosed greenschist facies basal juvenile tholeiitic basalts, effusive calc-alkaline basaltic magmatic rocks, 2139 ± 2 Ma [7] flysch-like sediments (composed of shales, siltstones and greywackes [7,11,12,17,22,37,63,72]; and chemical sediments defined by cherts and manganiferous sediments. These rocks have been intruded by large dome-shaped post-tectonic 2104 Ma granitoids [11,71]. The Koudougou-Tumu domain is composed of 2.16 to 2.13 Ga high-grade magmatic and felsic gneisses, ortho and *para*-gniesses, granitoids as well as gabbros. Intruding these rocks are the late 2.12 Ga granites [7,21,31]. The Bole-Bulenga domain comprises granulite facies paragneisses with migmatitic flows and metabasites. Intruding these rocks are the 2.19 Ga and 2.14 Ga granitoids [7, 22]. Overlying the Bole-Bulenga domain are the Tarkwaian-like sediments composed of quartzites, schist and garnetiferous schist. The polycyclic structural settings of NW Ghana described here are mainly based on the work of [11,12,22,63]. Several complex periodic

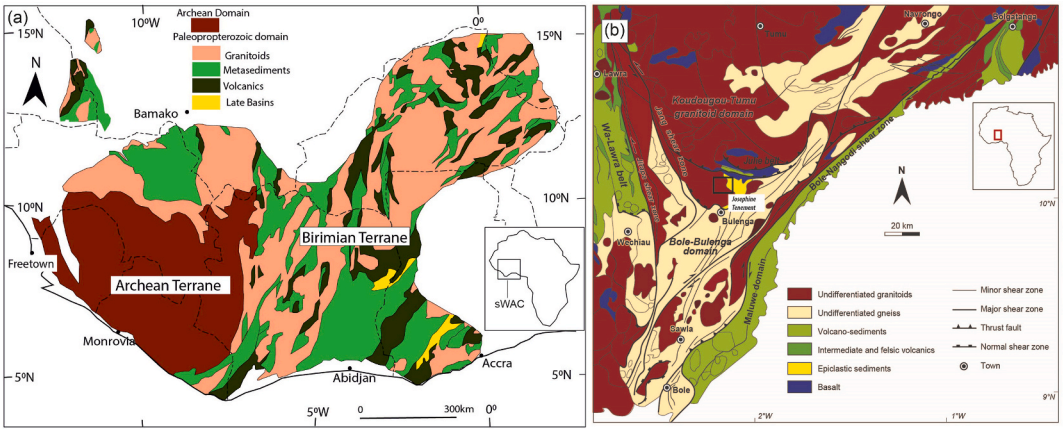

Fig. 2. (a) Simplified geological map of the southern portion of the West African craton (modified after Milési et al. (2004)) with the study area indicated with a red box. The pink colour indicates granitoids, with the light and deep green indicating volcanosedimentary and basaltic rock respectively, whiles the yellow indicate the Tarkwaian sediments (b) Simplified geological map of NW Ghana (modified after Block et al. (2016).

poly-deformational events have been recognized in NW Ghana. The initial sets of deformations (D1 - D3) happened circa 2144 to 2110 Ma and comprised a set of compressional and extensional tectonics. D4, the fourth deformational event is associated with sinistral Riedel shear zones. The last two deformational events (D6 - D7) are manifested by the late E-W brittle faults with cuts across all the previous deformations.

2.3. Mineralization style of the study area

The only available research work done on gold mineralization and structural setting in the Josephine tenement is work done by Ref. [18] and internal reports by Azumah Resources Limited [19]. Gold prospects on the Josephine PL Area in NW Ghana are hosted mainly in quartzites based on field mapping, aero-geophysical dataset interpretation, and drill core logging by Refs. [18,19], although other rocks such as granite, gabbro do exist on the tenement. The quartzites are grey and composed predominantly with preserved cross stratification. Metamorphic mineral assemblages defining these quartzites are chlorite mainly replacing the feldspar, magnetite and sulphides (thus arsenopyrites and pyrites). The summary of structural studies describing the structural controls on the auriferous quartz lodes on the tenement by Ref. [18] is defined by D0, D1, D2 and D3. D0 is mainly defined by the primary cross-stratification, while D1 is characterised by a north-northwestern (NNW) trending dextral shear zone with right-stepping dilatational jogs serving as sites for the precipitation of the gold mineralization on the tenement. The D1 shear zone is associated with steep to shallow dips, with the steeply dipping rocks associated with the footwall and that of the shallow dips associated with the hanging wall. The syn-tectonic quartz-carbonate-sulphide veins (lode) hosting the gold mineralization on the tenement are parallel to the D1 deformation on the Josephine tenement. D2 is characterised by open folds with axial planes striking NE-SW with dips ranging between 40 and 70. The final stage of deformation on the tenement is defined by NNE-SSW foliation which has obliterated most of the D1 and D2 deformational events on the tenement.

The most important wall rock alteration associated with gold prospects on the tenement is intense silicification which occurs mainly as bleached rocks. Besides silicification, other important alteration minerals that define the mineralization zone are chlorite, sericite, and sulphides. Native gold in the mineralized prospects on the tenement is associated mainly with arsenopyrite, pyrite, chalcopyrite and galena, but the main metallic mineral hosting the gold is the arsenopyrites. The gold within the quartz lodes occurs in arsenopyrite, or as free gold held as fissure filling enclosed within the arsenopyrite mineral.

3. Methodology

3.1. Construction of a geospatial dataset

The first step that is carried out during the creation of a predictive model that characterizes potential zones of mineral occurrences within an area of interest is the acquisition of essential geoscientific datasets. Thus, geological and geophysical datasets that had been acquired respectively by the Ghana Geological Survey Authority (GGSA) and Azumah Resources Limited (AZL) were obtained by the authors to generate predictive models that characterize potential areas of mineral occurrence within the Josephine prospective licence area of Northwestern Ghana [7,19]. The second step in mineral prospectivity modeling (MPM) is concerned with the extraction of appropriate thematic layers that are essential and viable towards the delineation of the target mineral within a chosen region [70]. In this regard, eight thematic layers were selected and derived from the acquired geological and high-resolution geophysical datasets (comprising magnetics and radiometrics) for employability in this study.

A detailed description, which highlights the basis upon which each of the eight geophysical- and geological-derived layers was chosen for the MPM is captured under Section 3.2. For magnetics, data was originally acquired in geodatabase (gdb) format. The magnetic data was first imported in the Geosoft Oasis Montaj software, where the total magnetic intensity (TMI) channel was gridded to generate the TMI grid. TMI grids in low magnetic latitude regions (including the Josephine PL Area) have their observed magnetic intensities asymmetric with their respective geological sources. In view of this, the reduction-to-equator (RTE) technique was applied to the TMI grid to generate an RTE layer, that symmetrically aligns the observed magnetic intensities with respect to the subsurface geological sources. The analytic signal filter was also applied to the TMI grid to produce the analytic signal layer. The lineament density layer, which characterizes the intensity of occurrence of delineated structural features such as fault, fractures, dikes, was also produced by applying the CET (Center for Exploration) grid analysis technique to the RTE grid. The radiometrics data, which was also in gdb format, was imported in Geosoft Oasis Montaj software, within which the potassium (K), equivalent thorium (eTh) and equivalent uranium (eU) channels were each gridded. The gridmath function in the Geosoft Oasis Montaj software was used to generate the potassium-thorium (K-eTh) ratio and uranium-thorium (eU-eTh) ratio grids. The geological data, that was obtained in vector format (polygon shapefile) was first converted to raster format to conform with the data type format of the geophysically extracted layers. By so doing, a geological thematic layer (made up of the main lithological classes within the study area) was obtained from the geological data. Thus, four radiometrically sourced layers (K, eU, K-eTh ratio and eU-eTh ratio), three magnetically-sourced layers (analytic signal, RTE and lineament density) as well as one geologically derived layer (geology) were chosen as the thematic layers for carrying out the MPM in this study. These eight thematic layers were subsequently imported into ArcGIS 10.4 for further processing and map-making. For the purpose of using the modeling methodologies, each of these thematic layers was rescaled in ArcGIS to a cell size of 5 m $\times$ 5 m, resulting in a total study area pixel count of 7608304. To conduct predictive modeling in a data-driven manner, known occurrence locations of the desired mineral are required. As a result, 144 known locations of gold (Au) occurrence (which depict regions with high Au geochemical anomalies in parts per billion as well as regions of artisanal mining operations) were identified together with their respective X and Y locations using geographic positioning systems (GPS) for

employability in this study. The 144 known locations of Au occurrences were similarly converted to pixels based on cell size of 5 m × 5 m, yielding a total Au occurrence pixel count of 3607. The 144 Au target locations (3607-pixel counts) were randomly divided into two comprising training data and testing data. The training data, which was used to train the MPM to be generated comprised 101 of the Au target data (2525-pixel counts, which is analogous to 70 % of the known location of Au occurrences). The testing data which also consists of 30 % of the total Au target locations (1082 pixel counts or 43 known locations) was used to evaluate and validate the efficacy of the predictive models produced. With the exception of the geological layer (Fig. 4(b)) whose source data comprises four classes, the seven other layers (analytic signal, lineament density, RTE, K, eU, K-eTh ratio and eU-eTh ratio) were characterized by continuous variables. In view of this, the Jenks natural breaking classification method was employed to discretize each of the seven thematic layers into suitable classes to aid in the determination of the spatial correlation between each thematic layer's class and the known Au occurrences within the study area [26,50]. Thus, the analytic signal (Fig. 3(a)), RTE layer (Fig. 3(b)), lineament density (Fig. 4(a)), uranium concentration (Fig. 5(a)), potassium concentration (Fig. 5(b)), uranium-thorium ratio (Fig. 5(c)) and potassium-thorium ratio (Fig. 5(d)) layers were respectively classified into six, seven, five, seven, eight, seven and seven classes respectively.

3.2. Details of geoscientific thematic layers created

The production of a mineral prospectivity model over the Josephine Prospecting Licence Area was contingent on the use of eight geoscientific thematic layers comprising analytic signal, lineament density, uranium-thorium ratio, uranium, potassium-thorium ratio, potassium, reduction-to-equator and geology. Each of these aforementioned thematic layers has been described in sub-subsections 3.2.1 to 3.2.5.

3.2.1. analytic signal thematic layer

The analytic signal thematic layer characterizes magnetic responses that are symmetric with respect to the sources that produce them (devoid of problems of asymmetry, associated with the total magnetic intensity responses over low latitude regions such as the study area). The analytic signal layer is also essential in identifying the boundaries of magnetic source bodies, in addition to structural attributes within the area under investigation [15,44,75]. With the study area mineralization associated with the presence of quartz-veins with disseminated sulphides (mainly arsenopyrite and pyrite, with minor pyrrhotite and chalcopyrite), regions characterized by high magnetic intensity gradient responses shown on the analytic signal layer (in Fig. 3(a)) could be attributed to the occurrence of indicator minerals such as arsenopyrite, magnetite and pyrite [45].

3.2.2. Reduction-to-equator thematic layer

The reduction-to-equator layer, which was generated by applying the reduction-to-equator filter on the total magnetic intensities over the study area mitigates asymmetric effects that arise when magnetic data is acquired in low magnetic latitude regions (such as the study area). Unlike the analytic signal which does not take into consideration the direction of magnetisation, the generation of the reduction-to-equator layer thrives primarily on the magnetic declination and inclination of the area concerned. Gold indicator minerals within the study area such as arsenopyrite, magnetite and pyrite are generally characterized by the high magnetic intensity zones within the reduction-to-equator layer (shown in Fig. 3(b)) [32,44,45].

3.2.3. lineament density thematic layer

The Center for Exploration Targeting (CET)-based lineament density thematic layer (shown in Fig. 4(a)) characterizes various

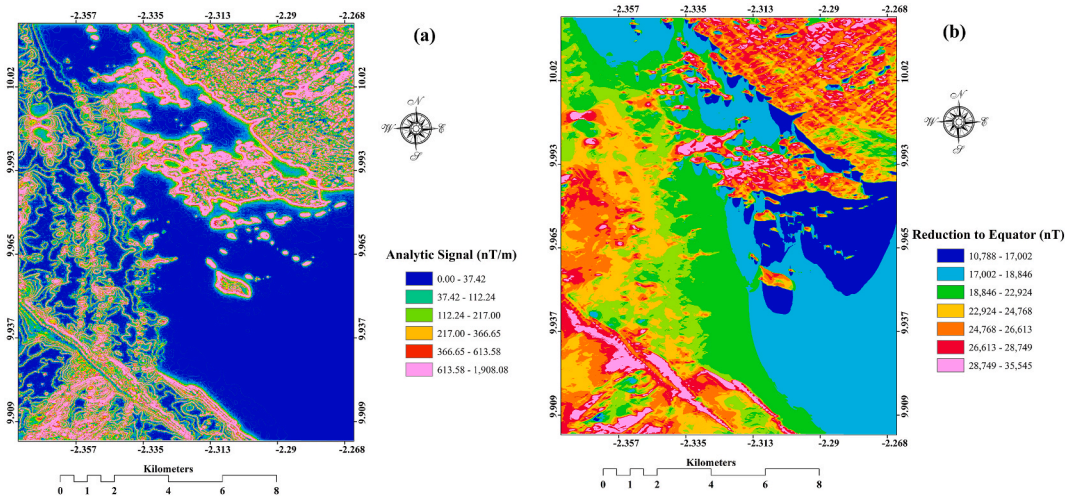

Fig. 3. Map of the classified (a) analytic signal layer (b) RTE-based magnetic intensity layer.

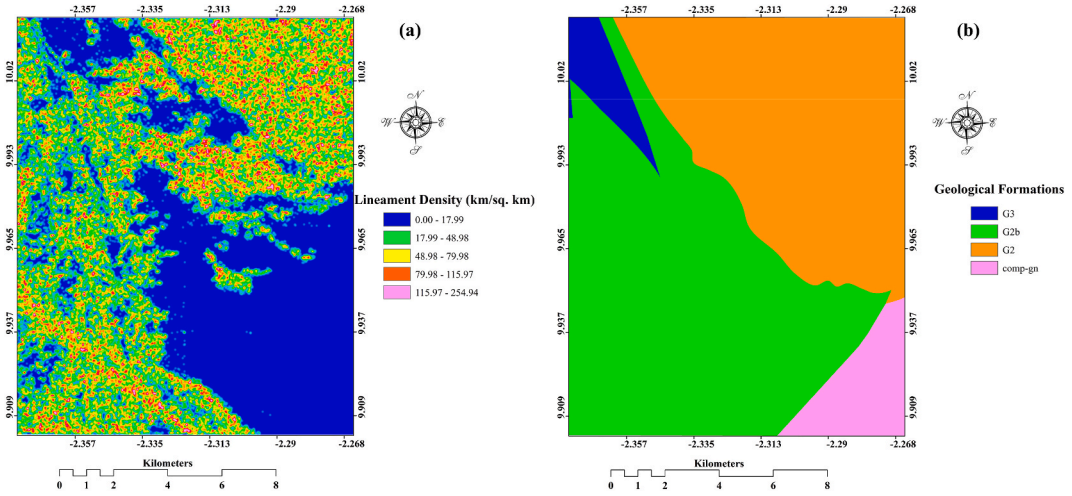

Fig. 4. Map of the classified (a) lineament density layer (b) geological layer.

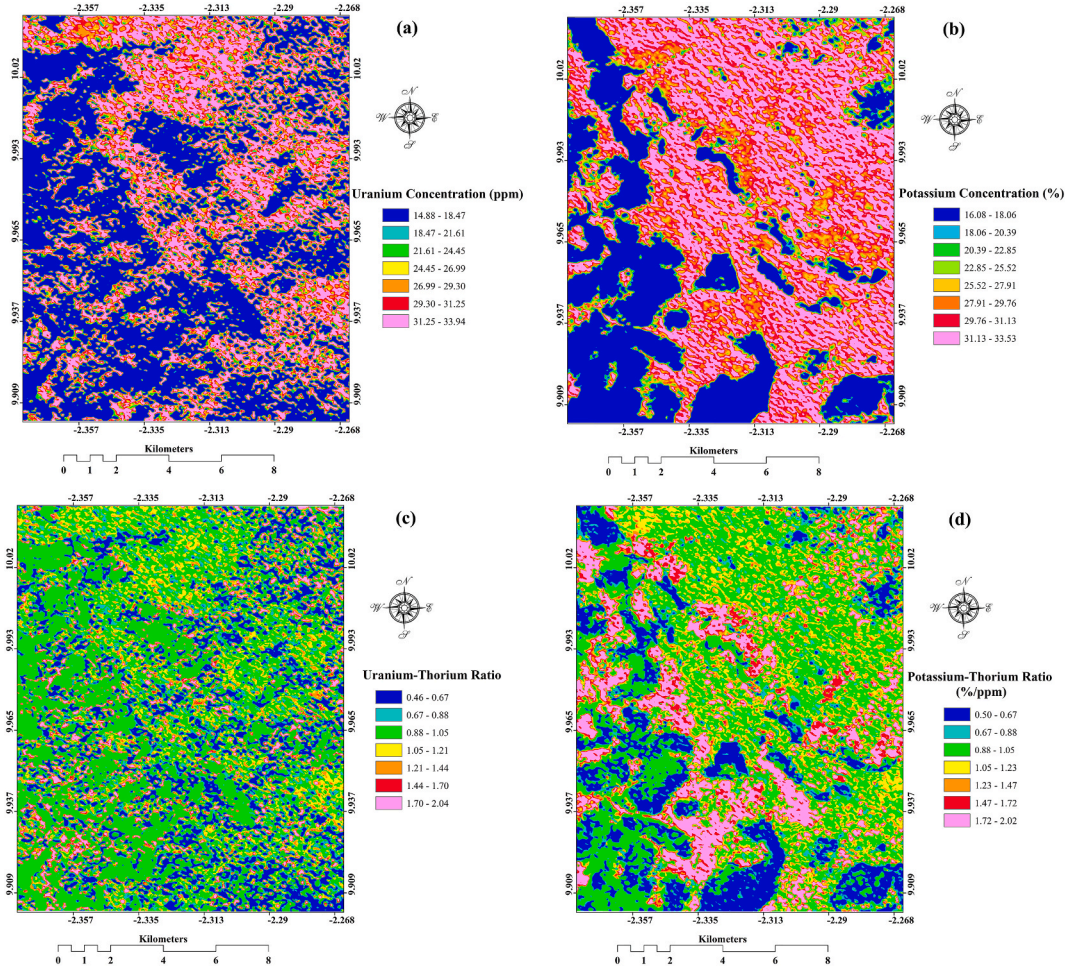

Fig. 5. Map of the classified (a) uranium concentration layer (b) potassium concentration layer (c) uranium-thorium ratio layer (d) potassium-thorium ratio layer.

regions with varying intensities of structural occurrences within the study area [13]. Thus, it concerns a particular region's structural endowment potential due to the occurrence of various geological structures or features. It is noteworthy that hydrothermal alteration zones with essential mineral prospects, primarily converge in regions where structural occurrence (fracturing) is intense [45]. Gold mineralization occurrence within the Josephine PL Area is primarily associated with quartz-veins (which depict the filling up of various cracks or fractures within rocks by minerals) and hence the use of the lineament density layer is an essential conditioning factor worthy of inclusion when generating a mineral prospectivity model over the study area [11,12,45].

3.2.4. Geological thematic layer

The rocks on the Josephine PL Area (shown in Fig. 4(b)) are composed of G3 (granodiorite batholiths), G2 (sheared granodiorite and diorites), G2b (granites, gabbros and schist) and comp-gn (composite gneisses composed of para- and ortho-gneisses). The granite, gabbro and schist in the Josephine PL Area have experienced intense NNW deformation, which is evidenced by a NNW striking shear foliation, with dips ranging from 40° to 80° and dip directions to the northeast. This NNW striking shear zone has experienced haloes of wall rock alteration which includes sulphidation, silicification and chloritization. Most of the gold mineralization in the study area is associated with milky, transposed quartz veins parallel to the shear foliation [11,12,18].

3.2.5. Radiometric thematic layers

Radiometric thematic layers are very essential in mineral prospecting owing to their ability to characterize classes of relevant radioelements vital for the delineation of various geological and alteration zones associated with mineralization within an area of interest [32,44]. It is important to note that alteration zones depict feasible zones with prospects of mineralization occurrence within an area. Thus, in this study, four radiometric thematic layers consisting of uranium concentration, potassium concentration, uranium-thorium ratio and potassium-thorium ratio were generated as shown respectively in Fig. 5(a), (b), 5(c) and 5(d). Regions that are enriched with uranium are deemed highly probable zones of mineralization occurrence. During the use of radiometrics for mineralization analysis, an increase in potassium concentration indicates possible gold mobilization within hydrothermal alteration systems. With regards to the K-eTh ratio, a decrease in thorium coupled with a corresponding increase in potassium suggests the possible prevalence of mineralization within the area of interest [44,81].

3.3. Mineral prospectivity modeling techniques

The data-driven based predictive models produced in this study were carried out using bivariate statistical models consisting of frequency ratio and information value.

3.3.1. Frequency ratio (FR) technique

The frequency ratio technique, a very straightforward bivariate statistical method, was used in this work to determine the spatial linkage between known Au occurrences and various classes of each selected theme layer. The application of the FR technique was based on the premise that, it has been found to be very useful for mapping out different zones of mineral occurrence [53], groundwater occurrence [10], flood susceptibility [43,73] and landslide vulnerability [1]. Mathematically, the frequency ratio for a chosen class i within a particular geoscientific thematic layer can be calculated based on the expression in equation (1).

$$FR_i = \frac{F_{TM}}{F_{AR}} = \frac{Au_i/Au_T}{AC_i/AC_T} \tag{1}$$

From equation (1), F_{TM} characterizes the Au occurrence frequency within class i of a given thematic layer; F_{AR} depicts the areal frequency of class i within a selected thematic layer; Au_i is the number of gold occurrences within class i of a given thematic layer; Au_T represents the total number of gold occurrences within all the classes in a given thematic layer; AC_i captures the areal size of class i and AC_T depicts the total areal size of a given thematic layer.

For a particular class i within a given thematic layer, a frequency ratio score of zero stipulates that there is no correlation between the said class i and gold occurrences within the study area. FR scores greater than 1, are an indication of a strong relationship between the gold occurrences and a given class of a given thematic layer. FR values less than 1, represent a weak correlation between various classes and gold occurrences. Using the frequency ratio approach for the development of an MPM in this study, each class within the eight geoscientific thematic layers were assigned their respective FR scores. After which, the prediction rate value scores obtained were multiplied by their respective thematic layers before synthesizing them to obtain the mineral prospectivity model. The predictive rate scores determine the overall contribution (weight) of each of the eight thematic layers towards the mineral prospectivity model produced as expressed in equation (2). A thematic layer with a PR score of 1 means, the said thematic layer's contribution towards the model generated is the least whereas those with high values are contributing highly towards the MPM produced.

$$PR_j = \frac{\left(\frac{FR_i}{\sum_{i=1}^{m} FR_i}\right)_{max} - \left(\frac{FR_i}{\sum_{i=1}^{m} FR_i}\right)_{min}}{\left[\left(\frac{FR_i}{\sum_{i=1}^{m} FR_i}\right)_{max} - \left(\frac{FR_i}{\sum_{i=1}^{m} FR_i}\right)_{min}\right]_{min}} \quad (2)$$

For a particular thematic layer j, PR_j is the predictive rate score obtained for that layer j; FR_i stands for the frequency ratio of the discrete classes within a given thematic layer and $\sum_{i=1}^{m} FR_i$ represents the summation of all frequency ratio values attained for all the categories within that thematic layer.

3.3.2. Information value (IV) technique

The information value (IV) technique, is a data-driven bivariate statistical method for predictive modeling in geoscience that was initially propounded by Ref. [83]. [78] modified this technique to reduce the complexities associated with its use in predictive modeling, particularly for geospatial mapping. The use of the information value technique primarily hinges on the concept that gold occurrence (Au_G) within a designated area of focus is related to various geoscientific features that are referred to as thematic layers (TM). The expression in equation (3) captures the theoretical basis upon which the information value technique was successfully

Table 1
Information Value and Frequency Ratio scores various classes of evidential layers used.

EVs	Class	Total Number of Pixels	Au occurrence pixels	IV	FR
Analytic Signal Layer (nT m−1)	0.00–37.42	4821927	1525	−0.0209	0.95
	37.42–112.24	1848453	600	−0.0096	0.98
	112.24–217.00	600711	225	0.0525	1.13
	217.00–366.65	227784	100	0.1215	1.32
	366.65–613.58	91256	50	0.2177	1.65
	613.58–1.908.08	18173	25	0.6175	4.15
Lineament Density Layer (km km−2)	0.00–17.99	2622254	1100	0.1017	1.26
	17.99–48.98	388703	200	0.1904	1.55
	48.98–79.98	611121	250	0.0908	1.23
	79.98–115.97	623103	350	0.2285	1.69
	115.97–254.94	3363123	625	−0.2518	0.56
Uranium Concentration Layer (ppm)	14.88–18.47	3272707	575	−0.2765	0.53
	18.47–21.61	281409	75	−0.0955	0.8
	21.61–24.45	400908	225	0.2279	1.69
	24.45–26.99	428088	125	−0.0559	0.88
	26.99–29.30	582099	300	0.1909	1.55
	29.30–31.25	923042	475	0.1902	1.55
	31.25–33.94	1720051	750	0.1183	1.31
Potassium Concentration Layer (%)	16.08–18.06	2041099	100	−0.8308	0.15
	18.06–20.39	159804	125	0.3723	2.36
	20.39–22.85	172891	25	−0.3608	0.44
	22.85–25.52	256768	25	−0.5326	0.29
	25.52–27.91	398344	100	−0.1212	0.76
	27.91–29.76	692986	375	0.2123	1.63
	29.76–31.13	1380288	375	−0.0869	0.82
	31.13–33.53	2506124	1400	0.2262	1.68
Uranium–Thorium Ratio Layer	0.46–0.67	1361495	300	−0.1782	0.66
	0.67–0.88	955845	350	0.0424	1.1
	0.88–1.05	3480740	1175	0.0071	1.02
	1.05–1.21	821283	275	0.0036	1.01
	1.21–1.44	434336	100	−0.1591	0.69
	1.44–1.70	224626	75	0.0023	1.01
	1.70–2.04	329979	250	0.3582	2.28
Potassium–Thorium Ratio Layer (%/ppm)	0.50–0.67	1095467	75	−0.6858	0.21
	0.67–0.88	584934	225	0.0638	1.16
	0.88–1.05	2943464	1000	0.0099	1.02
	1.05–1.23	1032376	575	0.2246	1.68
	1.23–1.47	520283	175	0.0055	1.01
	1.47–1.72	445726	75	−0.2953	0.51
	1.72–2.02	986054	400	0.0869	1.22
Geological Layer	G2b	3805174	1375	0.037	1.09
	comp-gn	508859	0	0	0
	G3	287085	0	0	0
	G4	3007186	1150	0.0616	1.15

adapted for usage in producing geospatial predictive models that characterizes probable precincts of mineral occurrence within the study area.

$$IV(Au_G, TM_i) = \log_2\left(\frac{P(Au_G, TM_i)}{P(Au_G)}\right) \quad (3)$$

where $IV\ (Au_G,\ TM_i)$ represents the information value score obtained for a given class i within a particular thematic layer TM; $P(Au_G)$ characterizes the probability of occurrence of Au mineral; and $P\ (Au_G,\ TM_i)$ captures the Au occurrence probability with respect to a given class i of a selected thematic layer (TM).

In the application of the information value modeling technique, IV scores obtained for each class of a given geoscientific thematic layer can either be positive, negative or zero. The scores obtained based on the use of the IV technique for each class i enable geospatial modelers to be able to establish the relationship between that class i and the Au occurrences. In view of this, a positive IV score means there is a strong association between the given class and the Au occurrences. Negative values of IV score characterize classes with a weak association towards gold occurrence within an area of focus. Zero values of IV score imply that, there is no correlation between the class of thematic layer and the Au occurrences. During the production of the IV-based MPM over the Josephine PL area, each class i within each of the eight thematic layers was assigned their respective IV scores before integrating them in a GIS environment.

3.4. Evaluation and validation of mineral prospectivity models

In geospatial predictive modeling, various models generated cannot be relied upon for any meaning deductions until they are evaluated and validated by scientifically acceptable validation tools [24,41]. Thus, validating models produced during a geospatial predictive modeling over an area of interest is very essential to building the confidence of geoscientists who would want to use the generated model for further deductions. In this study, the area under the receiver operating characteristics (AUC) curve was employed to validate the performance of the two mineral predictive models generated based on the frequency ratio and the information value techniques. In carrying out the AUC-based validation of the predictive models, the test data (30 % of total labels) were matched with the generated MPMs. The AUC curve generally comes with two axes; an x-axis along which the false positive rates are contained and a y-axis that characterizes the true positive rates. Though AUC curve score generally span from 0.5 to 1.0, score values closer to 1.0 (greater or equal to 0.7) are those that are deemed to indicate that the model produced is highly accurate.

4. Results and discussion

4.1. Geospatial analysis of thematic layers with respect to gold occurrences

In data-driven-based bivariate mineral predictive modeling, the geospatial relationship between various classes of a given geoscientific thematic layer with reference to the locations of mineral occurrences within the area of interest ought to be assessed. Hence, the use of two bivariate data-driven models comprising frequency ratio (FR) and information value (IV) was used to achieve the aforementioned task over the Josephine PL Area of northwestern Ghana (results shown in Tables 1 and 2). By utilizing the frequency ratio technique, each of the six classes within the analytic signal thematic layer was assessed to analyse their relationship to gold occurrences within the area of interest. The frequency ratio results obtained for the two analytic signal (AS) layer classes with magnetic intensity gradient values in the range of 0.00–37.42 nT/m and 37.42 nT/m - 112.24 nT/m were respectively 0.95 and 0.98. Also, the information value scores obtained for these aforementioned two analytic signal classes were respectively −0.0209 and −0.0096. A FR score of less than 1 and a negative IV score refer to a weak class-occurrence correlation. Thus, the AS classes with ranges 0.00–37.42 nT/m and 37.42 nT/m - 112.24 nT/m are weakly associated with known gold mineralization occurrences within the study area. The other four AS classes with class range values of 112.24 nT/m - 217.00 nT/m, 217.00 nT/m - 366.65 nT/m, 366.65 nT/m - 613.58 nT/m and 613.58 nT/m - 1.908.08 nT/m were observed to have FR scores (1.13, 1.32, 1.65 and 4.15) greater than 1 as well as positive IV scores (0.0525, 0.1215, 0.2177 and 0.6175 respectively). Hence, 112.24 nT/m, - 217.00 nT/m, 217.00 nT/m - 366.65 nT/m, 366.65 nT/m - 613.58 nT/m and 613.58 nT/m - 1.908.08 nT/m represent the AS layer classes with strong association towards gold mineralization occurrence within the study area. This result further indicates that classes (regions) with high magnetic intensity gradients are strongly associated with the known gold occurrences within the study area. This observation corroborates with literature and mineralization style of the study area, which encompasses the presence of magnetically high indicator minerals such as arsenopyrite,

Table 2
Information Value and Frequency Ratio scores various classes of evidential layers used Continued.

EVs	Class	Total Number of pixels	Au occurrence pixels	IV	FR
RTE Layer (nT)	10,788–17.002	405095	150	0.0476	1.12
	17.002–18.846	949815	100	−0.4986	0.32
	18,846–22,924	1257238	100	−0.6204	0.24
	22.924–24.768	1183821	175	−0.3512	0.45
	24,768–26,613	1152788	875	0.3593	2.29
	26,613–28,749	1773624	850	0.1596	1.44
	28,749–35,545	885923	275	−0.029	0.94

magnetite and pyrite within the area of interest [9,11,12].

For the five-classified lineament density thematic layer, only one class with a lineament density range of values of 115.97 km km^{-2}-254.94 km km^{-2} exhibited a weak association with the known mineral occurrences within the study area owing to the attainment of FR and IV scores of 0.56 and −0.2518 respectively. The other four lineament density classes with a range of values 0.00–17.99 km km^{-2}, 17.99 km km^{-2} - 48.98 km km^{-2}, 48.98 km km^{-2} - 79.98 km km^{-2} 79.98 km km^{-2} - 115.97 km km^{-2} were observed to have computed FR scores of 1.26, 1.55, 1.23 and 1.69 as well as IV scores of 0.1017, 0.1904, 0.0908 and 0.2285 respectively. FR and IV scores were also calculated for the uranium concentration layer, which had been discretized into seven classes as shown in Table 1. Three of the seven classes with uranium concentration value ranges of 14.88 ppm–18.47 ppm, 18.47 ppm–21.61 ppm and 24.45 ppm–26.99 ppm were seen to have their computed FR values less than 1 (0.53, 0.80 and 0.88 respectively) and negative IV scores of −0.2765, −0.0955 and −0.0559 respectively. This is an indication that these three Uranium concentration classes relate to the known gold occurrence within the area of interest in a weak manner. The other four uranium concentration classes had a range of concentration values comprising 21.61 ppm–24.45 ppm, 26.99 ppm–29.30 ppm, 29.30 ppm–31.25 ppm and 31.25 ppm–33.94 ppm respectively, with their computed frequency ratio scores being respectively 1.69, 1.55, 1.55 and 1.31. The information value scores for the aforementioned four uranium concentration classes were respectively 0.2279, 0.1909, 0.1902 and 0.1183, an indication of strong coherence between locations of known gold occurrences with respect to the aforementioned four uranium concentration classes. Inference from the results obtained for FR and IV scores also shows a general trend, where classes with higher uranium concentrations were observed to have a strong correlation to known gold occurrences within the study area; this also substantiates with what is reported in the literature that, regions of high uranium concentrations depict regions of possible gold mineralization occurrences [44,81]. In the case of the potassium concentration layer of eight classes, three of the classes with a potassium concentration of 18.06 ppm–20.39 ppm, 27.91 ppm–29.76 ppm and 31.13 ppm–33.53 ppm were observed to show a strong association in relation to the known gold occurrences within the area under study. The FR scores obtained for these three classes were respectively 2.36, 1.63 and 1.68 whereas the IV scores obtained were also 0.3723, 0.2123 and 0.2261 respectively. The other five classes, however, exhibited a weak association with the mineral occurrence within the area of interest with negative IV scores and FR values of less than 1. Also, the potassium concentration class with the highest range of concentration values also doubles as the class with the highest areal size among the classes (with class pixels of 2506124) was observed to exhibit a strong association with the gold occurrences, which corroborates with literature assertion that high potassium concentration is an indication of possible gold deposit mobilization within a hydrothermal alteration system [44].

In the case of the eU-eTh ratio layer, seven classes were observed. Only two uranium-thorium ratio classes with ratio values in the range of 0.46–0.67 and 1.21–1.44 were observed to show weak association with the gold occurrences within the study area with FR scores of 0.66 and 0.69 respectively and IV scores of −0.1782 and −0.1591 respectively. The other five eU-eTh ratio classes were observed to show a strong correlation to gold occurrence with the class having the highest ratio 1.70–2.04 also showing an FR score greater than 1 (2.28) as well as a positive IV score (0.3582). For the seven-classified K-eTh ratio thematic layer, two classes with ratio value ranges of 0.50 %/ppm - 0.67 %/ppm 1.47 %/ppm - 1.72 %/ppm were statistically analyzed to have FR scores of 0.21 and 0.51 respectively as well as IV scores of −0.6858 and −0.2953 respectively. This indicates that the known Au occurrences and the aforementioned classes have a weak spatial correlation within the study area. The other five classes of K-eTh ratio layer were statistically observed to be associated with positive IV scores with FR values greater than 1; which indicates that these classes (with class ranges of 0.67 %/ppm - 0.88 %/ppm, 0.88 %/ppm - 1.05 %/ppm, 1.05 %/ppm - 1.23 %/ppm, 1.23 %/ppm - 1.47 %/ppm and 1.72 %/ppm - 2.02 %/ppm) are strongly associated with variously identified sites of notable gold occurrences within the area of interest. In the reduction-to-equator (RTE) thematic layer, four classes with magnetic intensity value ranges of 17.002 nT–18.846 nT, 18,846 nT - 22,924 nT, 22.924 nT–24.768 nT, and 28,749 nT - 35,545 nT were characterized by computed frequency ratio scores less than 1 and negative IV scores. These FR and IV scores obtained presuppose that the said classes have a weak correlation with regards to gold

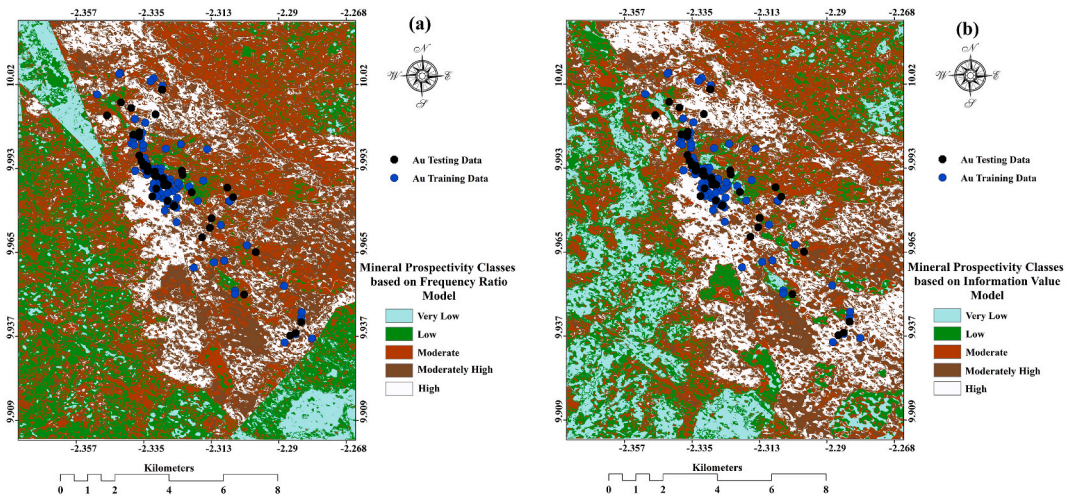

Fig. 6. (a) FR-based MPM (b) IV-based MPM.

occurrences within the area of interest. RTE classes with magnetic intensity ranges of 10,788 nT–17.002 nT, 24,768 nT, - 26,613 nT and 26,613 nT - 28,749 nT were observed to exhibit strong correlation to gold occurrence within the area of interest owing to the positive IV scores (0.0476, 0.3593 and 0.1596 respectively) as well as FR scores greater than 1 (1.12, 2.29 and 1.44 respectively) obtained for each of these three classes. At the instance of applying the frequency ratio and the information value techniques to the four-discretized geological layer, it was observed that, the comp-gn and G3 classes showed no correlation to gold occurrences within the area of interest because of the zero scores attained for both the frequency ratio and the information value techniques. The other two classes with geological symbols G2b and G2 were observed to exhibit a strong association with mineral occurrence within the area of interest due to the computed scores obtained for the FR and IV. For the frequency ratio, the scores obtained for the G2b and G2 classes were respectively 1.09 and 1.15 whereas the scores obtained for the classes upon the application of the information value technique were respectively 0.0370 and 0.0616.

4.2. Outputs of the mineral prospectivity modeling

The creation of mineral prospectivity models over the Josephine Prospecting Licence Area of the Northwestern part of Ghana was preceded by employing the scores obtained for the two data-driven statistical techniques comprising the frequency ratio and information value for each of the eight thematic layers used. Thus, the final output of the MPM developed based on the frequency ratio approach and the information value approach are respectively shown in Fig. 6(a) and (b); which were classified into five, and characterize regions of very low, low, moderate, moderately high and high prospective to gold mineralization occurrence within the area of interest. For the frequency ratio based mineral prospectivity model (FR-based MPM), the very low, low, moderate, moderately high and high prospective zones characterized respectively 6.5 %, 22.32 %, 28.36 %, 27.95 % and 14.86 % of the total study area size (shown in Table 3). In the case of the mineral prospectivity model generated based on the information value approach (IV-based MPM), regions delineated with very low, low, moderate, moderately high and high gold mineralization prospects made up of respectively 12.50 %, 18.96 %, 23.16 %, 25.67 % and 19.71 % of the total study area size. These high prospective zones in both the FR-based MPM and IV-based MPM are generally predominant in the northwestern, central, mid-central and mid-eastern portions of the study area with high potassium concentration, moderate to high K/eTh ratio, G2b lithology and high uranium concentration. The highly prospective zones (high class) within the northwestern and the north-central portions of the study area are also characterized by high lineament density and high magnetic intensity, which indicates the presence of intense structural features (quartz-veins) as well as gold-associated indicator minerals such as arsenopyrite, chalcopyrite and pyrite [11,12,18].

4.3. Accuracy assessment of generated mineral prospectivity models

Mineral prospectivity models produced cannot be deemed worthy or reliable until they have been evaluated to ascertain their accuracy. A predictive model, whose accuracy has been determined conveys confidence in the outputs generated by the models. In view of this, MPMs produced by employing the frequency ratio and the information value techniques were evaluated using the receiver operating characteristics (ROC) curve (as shown in Fig. 7(a) and (b)). On the horizontal axis of the ROC curves obtained for FR-derived MPM and IV-derived MPM is the false positive rate which describes an instance where a particular region is predicted to be prospective to gold mineralization, when that is not the case in reality. The vertical axis is referred to as the true positive rate, which also describes an instance where a region delineated as prospectively high is correctly predicted. The ROC scores obtained for the FR-derived MPM and IV-derived MPM were respectively 0.815 and 0.794. These ROC scores (both of which are greater than 0.7) obtained for each of the two models indicate that the models are efficiently derived. Notwithstanding, by comparing the two ROC scores obtained, it can be inferred that the mineral prospectivity model produced by employing the frequency ratio technique was more efficient than that of the information value technique.

5. Conclusion

In this study, two data-driven statistical approaches comprising the frequency ratio and information value techniques were used comparatively for the generation of mineral prospectivity models (MPMs). In particular, the aim of this study was to delineate the capacity of obtaining mineral prospectivity models over the Josephine PL Area of Northwestern Ghana by employing eight evidential layers sourced from airborne magnetic, airborne radiometric and geological datasets. The efficacy of the MPMs produced were evaluated using the area under the receiver operating characteristics curve which yielded analogously good predictive results with AUC scores of 0.794 and 0.815 respectively for the IV-derived MPM and FR-derived MPM. The frequency ratio model improved the overall predictive power and showed better performance than the MPM produced based on the information value approach. Thus, this study demonstrated the usefulness of the frequency ratio and information value data-driven statistical approaches in delineating potential zones of gold mineralization occurrence within the study area. It is therefore recommended that the mineral prospectivity models generated based on the IV and FR approaches be incorporated in assisting and planning future mineral exploration activities within the study area.

Declarations

We confirm that the manuscript has been read and approved by all named authors and that there are no other persons who satisfied the criteria for authorship but are not listed. We further confirm that the order of authors listed in the manuscript has been approved by

Table 3
Area extent and percentage of mineral prospectivity classes.

MPM Class	Information Value		Frequency Ratio	
	Area of class	Percentage	Area of class	Percentage
	(km2)	(%)	(km2)	(%)
Very Low	23.74	12.5	12.35	6.5
Low	36.01	18.96	42.39	22.32
Moderate	43.99	23.16	53.86	28.36
Moderately High	48.74	25.67	53.07	27.95
High	37.43	19.71	28.22	14.86

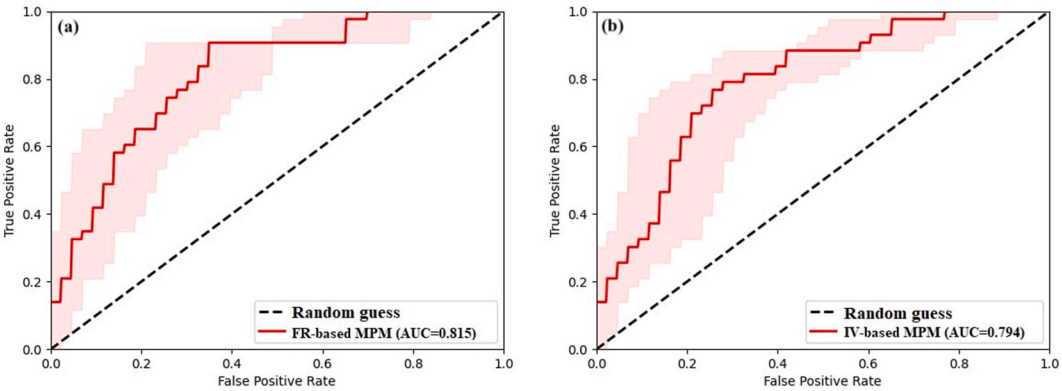

Fig. 7. ROC curves for the (a) FR-based MPM (b) IV-based MPM.

all of us.

Funding

No funding was received for this project.

Data availability statement

Data would be made available upon reasonable request.

CRediT authorship contribution statement

Eric Dominic Forson: Conceptualization, Formal analysis, Investigation, Methodology, Software, Validation, Visualization, Writing – original draft, Writing – review & editing. **Prince Ofori Amponsah:** Data curation, Formal analysis, Investigation, Writing – original draft, Writing – review & editing.

Declaration of competing interest

The authors declare that they have no known competing financial interests or personal relationships that could have appeared to influence the work reported in this paper.

Acknowledgement

The authors will like to that Azumah Resources Limited for allowing their tenement and data to be used for this exercise.

References

[1] H. Abdo, Assessment of landslide susceptibility zonation using frequency ratio and statistical index: a case study of al-fawar basin, tartous, Syria, Int. J. Environ. Sci. Technol. 19 (4) (2022) 2599–2618.
[2] M. Abedi, Electre iii: a knowledge-driven method for integration of geophysical data with geological and geochemical data in mineral prospectivity mapping? J. Appl. Geophys. 117 (2015) 138–140.

[3] M. Abedi, S.A. Torabi, G.-H. Norouzi, M. Hamzeh, Electre iii: a knowledge-driven method for integration of geophysical data with geological and geochemical data in mineral prospectivity mapping, J. Appl. Geophys. 87 (2012) 9–18.
[4] M. Abedi, S.A. Torabi, G.H. Norouzi, M. Hamzeh, G.R. Elyasi, Promethee II: a knowledge-driven method for copper exploration, Comput. Geosci. 46 (2012) 255–263.
[5] W. Abouchami, M. Boher, F. Albarede, 2.1 mafic magmatism in west africa: an early stage of crustal accreation, in: Seventh International Conference on Geochronology, Cosmochronology and Isotope Geology, 1990.
[6] Y. Achour, A. Boumezbeur, R. Hadji, A. Chouabbi, V. Cavaleiro, E.A. Bendaoud, Landslide susceptibility mapping using analytic hierarchy process and information value methods along a highway road section in constantine, Algeria, Arabian J. Geosci. 10 (8) (2017) 1–16.
[7] J. Agyei-Duodu, Geological Map of Ghana 1: 1 000 000, Geological Survey Department, 2009.
[8] A.M. Al-Abadi, Modeling of groundwater productivity in northeastern wasit governorate, Iraq using frequency ratio and shannon entropy models, Appl. Water Sci. 7 (2) (2017) 699–716.
[9] P.O. Amponsah, E.D. Forson, Geospatial modelling of mineral potential zones using data-driven based weighting factor and statistical index techniques, J. Afr. Earth Sci. 206 (2023), 105020.
[10] P.O. Amponsah, E.D. Forson, P.S. Sungzie, Y.S.A. Loh, Groundwater Prospectivity Modeling over the Akatsi Districts in the Volta Region of ghana Using the Frequency Ratio Technique, Modeling Earth Systems and Environment, 2023, pp. 1–19.
[11] P.O. Amponsah, S. Salvi, D. Béziat, L. Siebenaller, L. Baratoux, M.W. Jessell, Geology and geochemistry of the shear-hosted julie gold deposit, nw Ghana, J. Afr. Earth Sci. 112 (2015) 505–523.
[12] P.O. Amponsah, S. Salvi, B. Didier, L. Baratoux, L. Siebenaller, M. Jessell, P.M. Nude, E.A. Gyawu, Multistage gold mineralization in the wa-lawra greenstone belt, nw Ghana: the bepkong deposit, J. Afr. Earth Sci. 120 (2016) 220–237.
[13] T.Y. Amponsah, D.D. Wemegah, S.K. Danuor, E.D. Forson, Depth-based correlation analysis between the density of lineaments in the crystalline basement's weathered zones and groundwater occurrences within the Voltaian basin, Ghana, Geophys. Prospect. (2023) 1–15. https://doi.org/10.1111/1365-2478.13422.
[14] T.Y. Amponsah, S.K. Danuor, D.D. Wemegah, E.D. Forson, Groundwater potential characterisation over the voltaian basin using geophysical, geological, hydrological and topographical datasets, J. Afr. Earth Sci. 192 (2022), 104558.
[15] A. Ansari, K. Alamdar, A New Edge Detection Method Based on the Analytic Signal of Tilt Angle (Asta)for Magnetic and Gravity Anomalies, 2011.
[16] M. Arab Amiri, M. Karimi, A. Alimohammadi Sarab, Hydrocarbon resources potential mapping using evidential belief functions and frequency ratio approaches, southeastern saskatchewan, Canada, Can. J. Earth Sci. 52 (3) (2015) 182–195.
[17] D.K. Asiedu, M. Agoe, P.O. Amponsah, P.M. Nude, C.Y. Anani, Geochemical constraints on provenance and source area weathering of metasedimentary rocks from the paleoproterozoic (~ 2.1 ga) wa-lawra belt, southeastern margin of the west african craton, Geodin. Acta 31 (1) (2019) 27–39.
[18] F. Atanga, P.O. Amponsah, S. Nunoo, D. Kwayisi, E.D. Forson, T.M. Akabzaa, P.M. Nude, The geology and geochemistry of the Rhyacian Josephine gold deposit, Northwest Ghana, B. Appl. Earth Sci. (2023), https://doi.org/10.1080/25726838.2023.2260583.
[19] Azumah Resources Limited, The Julie Mineral Resource Estimate, 2018. Unpublished internal report.
[20] H. Bai, Y. Cao, H. Zhang, C. Zhang, S. Hou, W. Wang, Combining fuzzy analytic hierarchy process with concentration–area fractal for mineral prospectivity mapping: a case study involving qinling orogenic beltin central China, Appl. Geochem. 126 (2021), 104894.
[21] L. Baratoux, V. Metelka, S. Naba, M.W. Jessell, M. Grégoire, J. Ganne, Juvenile Paleoproterozoic crust evolution during the eburnean orogeny (2.2–2.0 ga), western Burkina Faso, Precambrian Res. 191 (1–2) (2011) 18–45.
[22] S. Block, M. Jessell, L. Aillères, L. Baratoux, O. Bruguier, A. Zeh, D. Bosch, R. Caby, E. Mensah, Lower crust exhumation during paleoproterozoic (eburnean) orogeny, nw Ghana, west african craton: interplay of coeval contractional deformation and extensional gravitational collapse, Precambrian Res. 274 (2016) 82–109.
[23] I. Bostjančic′, M. Filipovic′, V. Gulam, D. Pollak, Regional-scale landslide susceptibility mapping using limited lidar-based landslide inventories for sisak-moslavina county, Croatia, Sustainability 13 (8) (2021) 4543.
[24] H. Bourenane, M.S. Guettouche, Y. Bouhadad, M. Braham, Landslide hazard mapping in the constantine city, northeast Algeria using frequency ratio, weighting factor, logistic regression, weights of evidence, and analytical hierarchy process methods, Arabian J. Geosci. 9 (2) (2016) 1–24.
[25] E.J.M. Carranza, Geochemical Anomaly and Mineral Prospectivity Mapping in GIS, Elsevier, 2008.
[26] J. Chen, S. Yang, H. Li, B. Zhang, J. Lv, Research on geographical environment unit division based on the method of natural breaks (jenks), Int. Arch. Photogram. Rem. Sens. Spatial Inf. Sci. 3 (2013) 47–50.
[27] W. Chen, W. Li, E. Hou, Z. Zhao, N. Deng, H. Bai, D. Wang, Landslide susceptibility mapping based on gis and information value model for the chencang district of baoji, China, Arabian J. Geosci. 7 (11) (2014) 4499–4511.
[28] Y. Chen, W. Wu, Application of one-class support vector machine to quickly identify multivariate anomalies from geochemical exploration data, Geochem. Explor. Environ. Anal. 17 (3) (2017) 231–238.
[29] Y. Chen, W. Wu, Mapping mineral prospectivity using an extreme learning machine regression, Ore Geol. Rev. 80 (2017) 200–213.
[30] D. Davis, W. Hirdes, U. Schaltegger, E. Nunoo, U-pb age constraints on deposition and provenance of birimian and gold-bearing tarkwaian sediments in Ghana, west africa, Precambrian Res. 67 (1–2) (1994) 89–107.
[31] G. De Kock, R. Armstrong, H. Siegfried, E. Thomas, Geochronology of the birim supergroup of the west african craton in the wa-bolé region of west-central Ghana: implications for the stratigraphic framework, J. Afr. Earth Sci. 59 (1) (2011) 1–40.
[32] M. Dentith, S.T. Mudge, Geophysics for the Mineral Exploration Geoscientist, Cambridge University Press, 2014.
[33] K. Dickson, G. Benneh, A New Geography of ghana, Longman group uk limited, 1988.
[34] F.Z. Echogdali, S. Boutaleb, A. Bendarma, M.E. Saidi, M. Aadraoui, M. Abioui, M. Ouchchen, K. Abdelrahman, M.S. Fnais, K.S. Sajinkumar, Application of analytical hierarchy process and geophysical method for groundwater potential mapping in the tata basin, Morocco, Water 14 (15) (2022) 2393.
[35] A. Es-Smairi, B. El Moutchou, A. El Ouazani Touhami, M. Namous, R.A. Mir, Landslide susceptibility mapping using gis-based bivariate models in the rif chain (northernmost Morocco), Geocarto Int. (2022) 1–31.
[36] S. Esmaeiloghli, S.H. Tabatabaei, E.J.M. Carranza, S. Hosseini, Y. Deville, Spatially-weighted factor analysis for extraction of source-oriented mineralization feature in 3d coordinates of surface geochemical signal, Nat. Resour. Res. 30 (6) (2021) 3925–3953.
[37] X. Feng, E. Wang, P.O. Amponsah, J. Ganne, R. Martin, M.W. Jessell, Effect of pre-existing faults on the distribution of lower crust exhumation under extension: numerical modelling and implications for nw Ghana, Geosci. J. 23 (6) (2019) 961–975.
[38] X. Feng, E. Wang, J. Ganne, P. Amponsah, R. Martin, Role of volcano-sedimentary basins in the formation of greenstone-granitoid belts in the west african craton: a numerical model, Minerals 8 (2) (2018) 73.
[39] Z. Field, J. Miles, A. Field, Discovering Statistics Using R. Discovering Statistics Using R, 2012, pp. 1–992.
[40] A. Ford, J.M. Miller, A.G. Mol, A comparative analysis of weights of evidence, evidential belief functions, and fuzzy logic for mineral potential mapping using incomplete data at the scale of investigation, Nat. Resour. Res. 25 (1) (2016) 19–33.
[41] E.D. Forson, P.O. Amponsah, Mineral prospectivity mapping over the Gomoa Area of Ghana's southern Kibi-Winneba belt using support vector machine and naive bayes, J. Afr. Earth Sci. 206 (2023), 105024.
[42] E.D. Forson, A. Menyeh, Best worst method-based mineral prospectivity modeling over the Central part of the Southern Kibi-Winneba Belt of Ghana, Earth Sci. Informat. (2023), https://doi.org/10.1007/s12145-023-00999-5.
[43] E.D. Forson, P.O. Amponsah, G.B. Hagan, M.S. Sapah, Frequency ratio-based flood vulnerability modeling over the greater accra region of Ghana, Model. Earth Syst. Environ. (2023) 1–20.
[44] E.D. Forson, A. Menyeh, D.D. Wemegah, Mapping lithological units, structural lineaments and alteration zones in the southern kibi-winneba belt of Ghana using integrated geophysical and remote sensing datasets, Ore Geol. Rev. 137 (2021), 104271.
[45] E.D. Forson, A. Menyeh, D.D. Wemegah, S.K. Danuor, I. Adjovu, I. Appiah, Mesothermal gold prospectivity mapping of the southern kibi-winneba belt of Ghana based on fuzzy analytical hierarchy process, concentration-area (ca) fractal model and prediction-area (pa) plot, J. Appl. Geophys. 174 (2020), 103971.

[46] E.D. Forson, D.D. Wemegah, G.B. Hagan, D. Appiah, F. Addo-Wuver, I. Adjovu, F.O. Otchere, S. Mateso, A. Menyeh, T. Amponsah, Data-driven multi-index overlay gold prospectivity mapping using geophysical and remote sensing datasets, J. Afr. Earth Sci. 190 (2022), 104504.
[47] C. Fu, K. Chen, Q. Yang, J. Chen, J. Wang, J. Liu, Y. Xiang, Y. Li, H. Rajesh, Mapping gold mineral prospectivity based on weights of evidence method in southeast asmara, Eritrea, J. Afr. Earth Sci. 176 (2021), 104143.
[48] J. Hronsky, D.I. Groves, R.R. Loucks, G.C. Begg, A unified model for gold mineralisation in accretionary orogens and implications for regional-scale exploration targeting methods, Miner. Deposita 47 (4) (2012) 339–358.
[49] G. James, D. Witten, T. Hastie, R. Tibshirani, An Introduction to Statistical Learning, vol. 112, springer, New York, 2013, p. 18.
[50] G.F. Jenks, Generalization in statistical mapping, Ann. Assoc. Am. Geogr. 53 (1) (1963) 15–26.
[51] V. Khosravi, A. Shirazi, A. Shirazy, A. Hezarkhani, A.B. Pour, Hybrid fuzzy-analytic hierarchy process (ahp) model for porphyry copper prospecting in simorgh area, eastern lut block of Iran, Mining 2 (1) (2021) 1–12.
[52] N.T. Kien, V.T.H. Lien, P.L.H. Linh, N.Q. Thanh, et al., Landslide susceptibility mapping based on the combination of bivariate statistics and modified analytic hierarchy process methods: a case study of tinh tuc town, nguyen binh district, cao bang province, vietnam, J. Disaster Res. 16 (4) (2021) 521–528.
[53] K. Kusuma, S. Chaitanya, B. Guru, et al., Frequency ratio modelling using geospatial data to predict kimberlite clan of rock emplacement zones in dharwar craton, India, Int. J. Appl. Earth Obs. Geoinf. 74 (2019) 191–208.
[54] E. Lebrun, J. Miller, N. Thébaud, S. Ulrich, T.C. McCuaig, Structural controls on an orogenic gold system: the world-class siguiri gold district, siguiri basin, Guinea, west africa, Econ. Geol. 112 (1) (2017) 73–98.
[55] H. Li, X. Li, F. Yuan, S.M. Jowitt, M. Zhang, J. Zhou, T. Zhou, X. Li, C. Ge, B. Wu, Convolutional neural network and transfer learning based mineral prospectivity modeling for geochemical exploration of au mineralization within the guandian–zhangbaling area, anhui province, China, Appl. Geochem. 122 (2020), 104747.
[56] J. Li, Y. Zhang, Gis-supported certainty factor (cf) models for assessment of geothermal potential: a case study of tengchong county, southwest China, Energy 140 (2017) 552–565.
[57] T. Li, R. Zuo, Y. Xiong, Y. Peng, Random-drop data augmentation of deep convolutional neural network for mineral prospectivity mapping, Nat. Resour. Res. 30 (1) (2021) 27–38.
[58] N. Lin, Y. Chen, L. Lu, Mineral potential mapping using a conjugate gradient logistic regression model, Nat. Resour. Res. 29 (1) (2020) 173–188.
[59] E. Mansouri, F. Felzi, A.J. Rad, M. Arian, A comparative analysis of index overlay and TOPSIS (based on AHP weight) for iron skarn mineral prospectivity mapping, A case studyin Savian Area, Markazi Province, Iran, Bullet. Mineral Res. Explorat. 155 (155) (2017) 147–160.
[60] H. McFarlane, L. Ailleres, P. Betts, J. Ganne, L. Baratoux, M. Jessell, S. Block, Episodic collisional orogenesis and lower crust exhumation during the palaeoproterozoic eburnean orogeny: evidence from the sefwi greenstone belt, west african craton, Precambrian Res. 325 (2019) 88–110.
[61] J. Milési, J. Feybesse, P. Pinna, Y. Deschamps, H. Kampunzu, S. Muhongo, J. Lescuyer, E. Le Goff, C. Delor, M. Billa, et al., Geological map of africa 1: 10,000,000, sigafrique project, in: 20th Conference of African Geology, BRGM, Orléans, France, 2004, pp. 2–7.
[62] M. Mohammadpour, A. Bahroudi, M. Abedi, Three dimensional mineral prospectivity modeling by evidential belief functions, a case study from kahang porphyry cu deposit, J. Afr. Earth Sci. 174 (2021), 104098.
[63] S. Nunoo, A. Hofmann, J. Kramers, Geology, zircon u–pb dating and ϵhf data for the julie greenstone belt and associated rocks in nw Ghana: implications for birimian-to-tarkwaian correlation and crustal evolution, J. Afr. Earth Sci. 186 (2022), 104444.
[64] J.W. Osborne, What is rotating in exploratory factor analysis? Practical Assess. Res. Eval. 20 (1) (2015) 2.
[65] M. Parsa, A. Maghsoudi, Assessing the effects of mineral systems-derived exploration targeting criteria for random forests-based predictive mapping of mineral prospectivity in ahar-arasbaran area, Iran, Ore Geol. Rev. 138 (2021), 104399.
[66] K. Pazand, A. Hezarkhani, M. Ataei, Using topsis approaches for predictive porphyry cu potential mapping: a case study in ahar-arasbaran area (nw, Iran), Comput. Geosci. 49 (2012) 62–71.
[67] S. Perrouty, L. Aillères, M.W. Jessell, L. Baratoux, Y. Bourassa, B. Crawford, Revised eburnean geodynamic evolution of the gold-rich southern ashanti belt, Ghana, with new field and geophysical evidence of pre-tarkwaian deformations, Precambrian Res. 204 (2012) 12–39.
[68] S. Radhakrishnan, R. Ramachandran, G. Murali, N.I. Vatin, A hybrid spatial–analytical network process model for groundwater inventory in a semi-arid hard rock aquifer system?a case study, Water 14 (17) (2022) 2743.
[69] G. Reza, A. Maghsoudi, A. Bigdeli, E.J.M. Carranza, Regional-scale mineral prospectivity mapping: support vector machines and an improved data-driven multi-criteria decision-making technique, Nat. Resour. Res. 30 (2021) 1977–2005.
[70] S. Riahi, A. Bahroudi, M. Abedi, S. Aslani, G.-R. Elyasi, Integration of airborne geophysics and satellite imagery data for exploration targeting in porphyry cu systems: chahargonbad district, iran, Geophys. Prospect. 69 (5) (2021) 1116–1137.
[71] P.A. Sakyi, B.-X. Su, S. Anum, D. Kwayisi, S.B. Dampare, C.Y. Anani, P.M. Nude, New zircon 605 u–pb ages for erratic emplacement of 2213–2130 ma paleoproterozoic calc-alkaline i-type granitoid rocks in the lawra volcanic belt of northwestern Ghana, west africa, Precambrian Res. 254 (2014) 149–168.
[72] M.S. Sapah, J.E. Agbetsoamedo, P.O. Amponsah, S.B. Dampare, D.K. Asiedu, Neodymium 608 isotope composition of palaeoproterozoic birimian shales from the wa-lawra belt, north-west Ghana: constraints 609 on provenance, Geol. J. 56 (4) (2021) 2072–2081.
[73] S. Siahkamari, A. Haghizadeh, H. Zeinivand, N. Tahmasebipour, O. Rahmati, Spatial prediction of flood-susceptible areas using frequency ratio and maximum entropy models, Geocarto Int. 33 (9) (2018) 927–941.
[74] T. Sun, K. Wu, L. Chen, W. Liu, Y. Wang, C. Zhang, Joint application of fractal analysis and weights-of-evidence method for revealing the geological controls on regional-scale tungsten mineralization in southern jiangxi province, China, Minerals 7 (12) (2017) 243.
[75] Y. Ting-Jie, W. Yan-Gang, Y. Yuan, C. Ling-Na, Edge detection of potential field data using an enhanced analytic signal tilt angle, Chin. J. Geophys. 59 (4) (2016) 341–349.
[76] M. Tsangas, M. Jeguirim, L. Limousy, A. Zorpas, The application of analytical hierarchy process in combination with pestel-swot analysis to assess the hydrocarbons sector in Cyprus, Energies 12 (5) (2019) 791.
[77] F.J. van Ruitenbeek, J. Goseling, W.H. Bakker, K.A. Hein, Shannon entropy as an indicator for sorting processes in hydrothermal systems, Entropy 22 (6) (2020) 656.
[78] C.J. Van Westen, Application of Geographic Information Systems to Landslide Hazard Zonation, 1993.
[79] M. Villeneuve, J. Cornée, Structure, evolution and palaeogeography of the west african craton andbordering belts during the neoproterozoic, Precambrian Res. 69 (1–4) (1994) 307–326.
[80] J. Wang, R. Zuo, Y. Xiong, Mapping mineral prospectivity via semi-supervised random forest, Nat. Resour. Res. 29 (1) (2020) 189–202.
[80a] Q. Wang, Y. Guo, W. Li, J. He, Z. Wu, Predictive modeling of landslide hazards in wen county, northwestern China based on information value, weights-of-evidence, an certainty factor, Geomatics, Nat. Hazards Risk 10 (1) (2019) 820–835.
[81] D.D. Wemegah, K. Preko, R.M. Noye, B. Boadi, A. Menyeh, S.K. Danuor, T. Amenyoh, et al., Geophysical interpretation of possible gold mineralization zonesin kyerano, south-western Ghana using aeromagnetic and radiometric datasets, J. Geosci. Environ. Protect. 3 (4) (2015) 67.
[82] Y. Xiong, R. Zuo, Recognizing multivariate geochemical anomalies for mineral exploration by combining deep learning and one-class support vector machine, Comput. Geosci. 140 (2020), 104484.
[83] K. Yin, T. Yan, Statistical prediction models for instability of metamorphosed rocks, in: International Symposium on Landslides, vol. 5, 1988, pp. 1269–1272.
[84] S. Yousefifar, A. Khakzad, H.A. Harooni, J. Karami, M. Jafari, M.V. Abedin, Prospecting of au 638 and cu bearing targets by exploration data combination in southern part of dalli cu-au porphyry deposit, central 639 Iran, Arch. Min. Sci. 56 (1) (2011) 21–34.